# Measurement and modeling of dispersive pulse propagation in drawn wire waveguides

Eric I. Madaras
*NASA Langley Research Center, Hampton, Virginia 23681-0001*

Thomas W. Kohl and Wayne P. Rogers
*University of Colorado, Department of Mechanical Engineering, Boulder, Colorado 80309-0427*

(Received 20 October 1993; accepted for publication 12 July 1994)

An analytical model of dispersive pulse propagation in semi-infinite cylinders due to transient axially symmetric end conditions has been experimentally investigated. Specifically, the dispersive propagation of the first axially symmetric longitudinal mode in thin wire waveguides, which have ends in butt contact with longitudinal piezoelectric ultrasonic transducers, is examined. The method allows for prediction of a propagated waveform given a measured source waveform, together with the material properties of the cylinder. Alternatively, the source waveform can be extracted from measurement of the propagated waveform. The material properties required for implementation of the pulse propagation model are determined using guided wave phase velocity measurements. Hard tempered aluminum 1100 and 304 stainless steel wires, with 127, 305, and 406 $\mu$m diam, were examined. In general, the drawn wires were found to behave as transversely isotropic media.

PACS numbers: 43.35.Pt, 43.20.Jr

## INTRODUCTION

Historically, pulse propagation in thin cylindrical waveguides has been of interest for applications including the material testing of wires and fibers,[1–3] ultrasonic delay lines,[4] medical ultrasonics,[5] and embedded sensor materials.[6] Propagation of ultrasonic waves in cylinders has been the subject of several investigations, both analytical and experimental.[7–20] In high-frequency and broadband applications, these cylinders may exhibit considerable dispersion when an acoustic pulse propagates through the waveguide. Here, dispersion is the dependence of acoustic guided wave phase velocity on frequency, resulting in distortion of the waveform of a transient plane-wave pulse depending on the axial location. This pulse distortion can make the interpretation of measured waveforms difficult. The present paper combines experimental measurements and analytical modeling to yield a quantitative and integrated approach to address the problem of pulse dispersion in cylindrical waveguides. The method presented also has significant relevance to the problem of material characterization of these waveguides.

## I. PULSE PROPAGATION

While exact[7–9] and approximate[10,11] solutions have been used to study the axially symmetric guided wave phase velocity versus frequency relationship in solid cylindrical waveguides, and experimental dispersion measurements have corroborated the theory,[12–15] few studies have been done to assess the capability these solutions yield for modeling actual pulse propagation. The earliest analytical solution, using exact theory, to the problem of axially symmetric pulse propagation in a cylindrical waveguide due to application of a transient end condition can be attributed to Skalak.[16] A special solution was obtained to the problem of a solid isotropic cylinder with a velocity imparted uniformly to the cylinder end in the form of a step function. Subsequently, Folk *et al.*[17] used exact theory to obtain a solution for a solid isotropic cylinder with arbitrary time harmonic mixed (combined displacement and stress) end boundary conditions. Moreover, an attempt was made by Folk *et al.*[17] to experimentally validate the solution in terms of its ability to model pulse propagation. Studies by Miklowitz and Nisewanger,[18] Hseih and Kolsky,[19] and McNiven and Mengi[20] have attempted to experimentally validate propagation models based on approximate theories. Only qualitative agreement between theoretical and measured waveforms was obtained in these studies. Furthermore, the pulses examined in all of these studies were dominated by lower-frequency propagation of the first longitudinal mode. The pulses, resulting from either ideal or modified (some finite rise time) step loading, essentially consist of a low-frequency leading head and a higher-frequency dispersive tail. While the current study also addresses first longitudinal mode propagation, the transient end conditions applied give rise to more varied dispersive pulse distortion. The frequency range considered extends from low frequency, where the fundamental tends toward nondispersiveness, to approaching the second longitudinal mode cutoff, where the fundamental becomes highly dispersive. An integrated analytical and experimental study of isotropic hollow cylinders using the same numerical method and similar measurement techniques[21] involves the propagation of higher-order longitudinal modes.

## II. PROPERTY MEASUREMENT

Because the dispersion of the guided waves depends on the elastic properties, cylindrical guided wave propagation has been used for the material characterization and testing of wires and fibers. Meeker and Meitzler[22] suggested several

 0001-4966/95/97(1)/252/10/$6.00  

methods for determining material properties by measuring acoustic guided wave velocities, and a thorough review of the subject has been given by Curtis.[1]

Principally, velocity measurements of the first torsional mode and the long wavelength limit of the first longitudinal mode have been used to obtain the shear and Young's moduli, respectively, for isotropic cylinders.[1,2] The first axisymmetric torsional mode is nondispersive, propagating at the shear wave velocity $(G/\rho)^{1/2}$. In the long wavelength (low-frequency) limit, the velocity of the first longitudinal axisymmetric mode tends toward the bar velocity $(E/\rho)^{1/2}$. As the limit is approached, group and phase velocities tend toward a constant and equal value, indicating nondispersive behavior.

However, the drawing process in the manufacture of wires and fibers can affect the material microstructure, frequently causing the material to be anisotropic.[1] Transverse isotropy, with five independent elastic constants, is considered to better represent the state of the material than isotropy. The five independent elastic properties for transversely isotropic media are taken as $E_{LL}$, $E_{TT}$, $G_{LT}$, $G_{TT}$, $\nu_{LT}$, where $E$, $G$, and $\nu$ are Young's moduli, shear moduli, and poisson ratio, respectively, L is longitudinal, and T is transverse.[23] Moreover, the propagation of the fundamental longitudinal mode, within the frequency range considered, does not depend on the transversely isotropic property to which the lowest torsional mode is sensitive, $G_{LT}$. Rather, the strongest dependence is on $E_{LL}$ and $\nu_{LT}$.

Longitudinal mode measurement to obtain $E_{LL}$ can be problematic. When the velocity of the long wavelength limit is used, a transient pulse with sufficient low-frequency content is propagated and its first arrival measured. Since the longest wavelengths of the first longitudinal mode propagate with greatest velocity, this time-of-flight measurement yields the velocity of the long wavelength limit. However, the leading head of a dispersive pulse often rises very gradually making accurate assessment of when the first arrival occurs difficult, as discussed by Curtis,[1] and evident in the low-frequency experimental waveforms of other studies.[17–20] Consequently, the measurement may be subject to some error. Instead, the time shift between the peak of the wave envelope of a propagated broadband pulse is often matched with that of the initial pulse.[2] However, the frequency and wavelength of such a velocity measurement is not at all clear.[24]

Alternatively, phase or group velocity of particular cylindrical guided wave modes can be measured over a range of frequency. Material properties are then varied to obtain correspondence between theoretical velocities and the dispersion measurements. As noted by Meeker and Meitzler,[22] dispersion measurements of the first axially symmetric longitudinal mode are sufficient to find both elastic constants for isotropic media. As will be illustrated here, combination of such measurement with measures of first torsional mode velocity yields $E_{LL}$, $\nu_{LT}$, and $G_{LT}$ for transversely isotropic media. The extent of the material anisotropy can then be gauged.

Phase velocity measurement methods are preferred to group velocity measurement methods since the wave propagation is generally dispersive. Inherent difficulty in group velocity measurements for dispersive media has been noted.[24,25] The problem stems from the distortion of the propagated waveform relative to the initially generated waveform and the resulting ambiguity in correlating the two different waveforms, and also, in determining the frequency for which the group velocity is being measured. Correspondingly, precision and accuracy for phase velocity measurement can be expected to exceed that obtained for group velocity measurement for dispersive pulse propagation. The scatter of group velocity measurements which commonly occurs for propagation in dispersive media can be seen in a recent study of sound in wires by Nicholson *et al.*[15] The precision of the measurement and smoothness of the curve determined by these measurements is critical to accurate and repeatable material property characterization. The elastic properties determined from the phase velocity measurements are used here as input to the pulse propagation model.

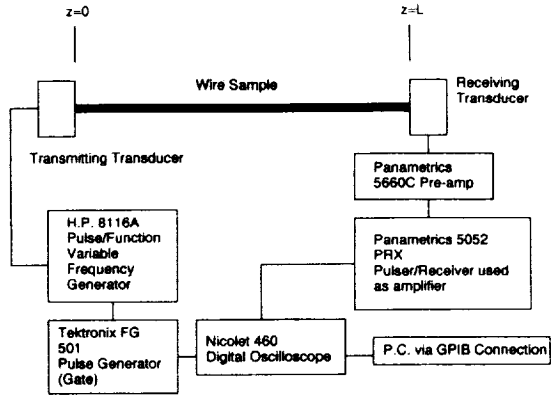


FIG. 1. Experimental apparatus.

## III. WAVE EXCITATION AND MEASUREMENT

The method by which elastic pulses are launched into the wire specimens and measured after propagating the length of the sample is illustrated in Fig. 1. Similar techniques have been used in other studies of ultrasound propagation in wires.[15] As shown in Fig. 1, matched pairs of piezoelectric longitudinal or shear wave transducers are placed in butt contact with each end of the wire and operate in pitch catch mode. For this study, 5 MHz center frequency panametrics V109 (longitudinal) and V156 (shear) transducers were used. Glycerin was used as couplant to aid in sound transmission across the transducer/wire interface. The source or excitation transducer was provided a gated sine wave or toneburst electrical signal. Because of the thinness of the wires, the efficiency at which sound could be introduced into the waveguides was very low. Consequently, gain in the receiving system between 60 and 100 dB was required and signal averaging between 300 and 600 data records was performed to improve signal to noise. Signals were captured and averaged on a digital oscilloscope and processed on a PC.

With longitudinal wave transducers in use, the pulse launched in the medium would be composed primarily of the first axially symmetric longitudinal mode. However, depending on factors such as the wire thickness, excitation fre-

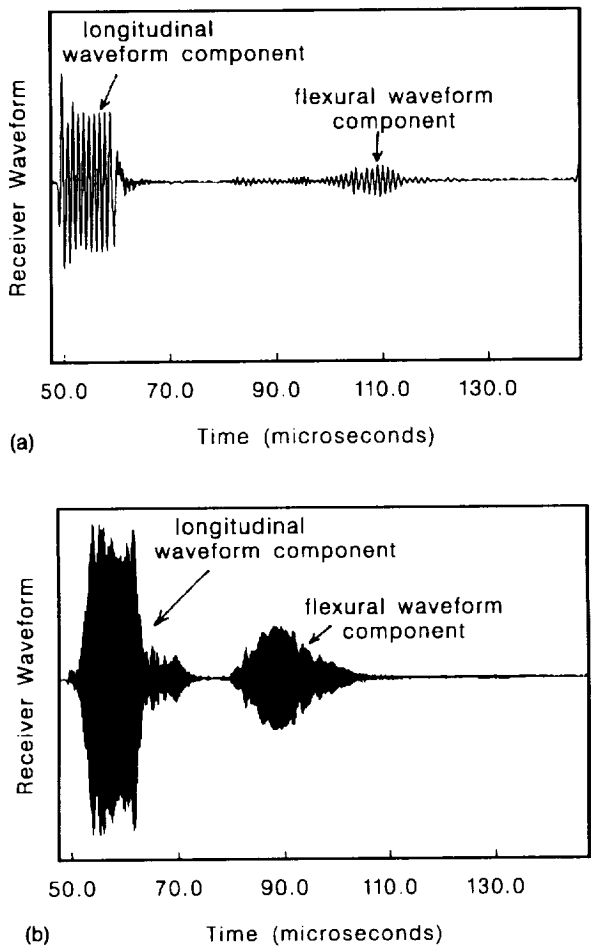


FIG. 2. Measured propagated pulse in a 24.76-cm-long, 12-mil-diam aluminum 1100 wire due to excitation of longitudinal piezoelectric source transducer with 1-MHz (top) and 5-MHz (bottom) tonebursts.

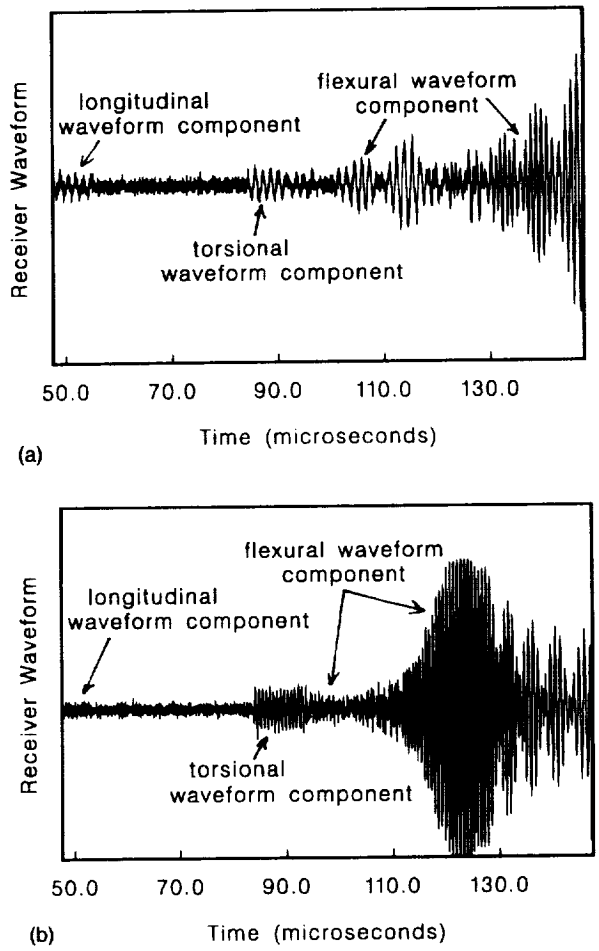


FIG. 3. Measured propagated pulse in a 25.22-cm-long, 5-mil-diam 304 stainless steel wire due of excitation to shear piezoelectric source transducer with 700-kHz (top) and 1.5-MHz (bottom) tonebursts.

quency, couplant effects, and obviously the contact between source transducer and wire, the first-order flexural mode was also excited. In general, the flexural mode propagates much more slowly than the axisymmetric longitudinal mode. Consequently, the waveform due to each of the two modes can be temporally separated after some length of propagation. However, with increasing frequency, the dispersion of the waveguide is such that the first longitudinal mode is observed to propagate more slowly while the flexural mode is observed to propagate faster. Propagation of higher-frequency harmonics may result in overlap and interference between axially symmetric longitudinal and nonsymmetric flexural waveform components. The longitudinal and flexural components of typical measured waveforms for bursts with increasing center frequency are shown in Fig. 2. Longitudinal wave transducers are used for generating and receiving the wave. The waveform component associated with the flexural mode was eliminated through windowing for both the phase velocity measurements and the extraction of the source signal from a measured received waveform.

Torsional modes were excited by using shear wave transducers and intentionally placing only an edge of the wire end into contact with the source transducers face. As a result of such contact, both longitudinal and torsional axisymmetric modes and at least first-order flexural modes were excited. By varying the frequency of the toneburst excitation of the shear wave transducer, and observing which wave packet remained fixed with regard to arrival and did not distort relative to the source waveform (nondispersive), the torsional wave packet could be identified. Torsional wave packets are shown for bursts of 0.7 and 1.5 MHz in Fig. 3. Since dispersive first-order flexural waves are also excited, caution must be used as flexural waves will often propagate at similar velocities relative to torsional waves. Consequently there is overlap of the waveforms over broad ranges of frequency. In Fig. 3, the faster propagation of the flexural mode when a higher-frequency burst was used, results in the beginning of interference between the nondispersive torsional mode and the highly dispersive flexural mode.

Source measurements were performed by placing the matched transducers into face to face contact without the intervening wire. It should be noted that source measurement by this method is imperfect since it neglects all transducer/wire interface effects. In particular, some variation in the behavior of the source transducer when electrically excited in unloaded (with wire contacting transducer face) as opposed to loaded (matched transducer face-to-face contact) condition could be anticipated. The effect of multiple reflections be-

tween the two transducer faces on the source signal measurement was also neglected.

## IV. BOUNDARY CONDITIONS AND ANALYTICAL MODELING

The cylinder end boundary conditions used in the analytical modeled, implemented here, approximate the test configuration of Fig. 1. The longitudinal source transducer is modeling as a piston source in smooth contact with the cylinder end. The boundary conditions applied are a time dependent pure axial pressure pulse $p(t)$ and vanishing shear stresses acting on the cylinder end surface. On the surface at $z=0$ then, normal traction is uniform $[p_z=p(t)]$ and shear tractions are zero $(p_r=p_\theta=0)$. Because the entire cylinder end is idealized to be in uniform contact with the longitudinal transducer, only axially symmetric mode excitation and propagation is modeled. Since flexural waves are excited experimentally, as was shown in Fig. 2, the model boundary conditions do not fully characterize the actual physical end conditions. However, assuming the end conditions can be decomposed into axially symmetric and nonsymmetric parts, it should be of great utility to develop a capability for both receiver waveform prediction and source waveform extraction based on the axially symmetric wave propagation, without necessarily characterizing the nonsymmetric part of the boundary conditions.

In a previous paper,[26] a solution for the problem of a time varying uniform (across the end face) axial displacement pulse in combination with (1) vanishing shear stresses and (2) vanishing circumferential and radial displacements, was given. The analytical development given in Kohl *et al.*,[26] is generalized in the current paper to boundary condition problems involving any well posed combination of prescribed axially symmetric, transient distributed forces or discretized displacements, specified at the cylinder end. The specific aforementioned boundary conditions, modeling the butt contact of a longitudinal ultrasonic transducer, give rise to a pure stress boundary condition.

The numerical method to be described has diverse application. The method is readily applicable to problems involving both solid and hollow cylindrical waveguides. Furthermore, the media of the waveguides need not be isotropic or homogeneous. A solution for problems involving anisotropic and radially inhomogeneous cylinders, such as filament wound composites, can be obtained. For conciseness, the development here follows directly from that given in Kohl *et al.*,[26] with only new formulation presented. Discussion in Kohl *et al.*[26] also provides further details on implementation of the modeling.

The eigenproblem of Eq. (3) in Kohl *et al.*[26] constitutes numerical solution for both the mode phase velocity dispersion relation, and the mode shapes or particle displacement distribution for each mode within the plane of the advancing wavefront. The integrations involved in the formation of the matrices of Eq. (3)[26] can be evaluated exactly except for $[k_3]$ which has a singularity at the center of a solid cylinder. Either Gaussian numerical integration or introduction of a pinhole to the center of the cylinder are satisfactory techniques for dealing with this singularity.

A variational formulation is used to determine the end condition equation governing the modal amplitudes $A_n$. Application of the principle of virtual work yields

$$\int_A (\sigma_{rz}\delta u_r+\sigma_{\theta z}\delta u_\theta+\sigma_{zz}\delta u_z)dA$$

$$=\int_A (p_r\delta u_r+p_\theta\delta u_\theta+p_z\delta u_z)dA, \tag{1}$$

where $p_i$ are the prescribed distributed forces acting on the cylinder end, $u_i$ are the displacements, and $\sigma_{ij}$ are the stresses. Equation (1) is applied to each element in the radially discretized system, yielding for the $k$th element

$$[\delta A]^T[Q]^{(k)^T}\int_{r_b}^{r_f}[N]^T[C^*]^{(k)}([b][Q']^{(k)}+[a][Q]^{(k)})r$$

$$\times dr\{A\}=[\delta A]^T[Q]^{(k)^T}\int_{r_b}^{r_f}[N]^T\{p\}r\,dr, \tag{2a}$$

where

$$[C^*]^{(k)}=\begin{bmatrix} 0 & 0 & 0 & 0 & C_{55} & C_{56} \\ C_{14} & C_{24} & C_{34} & C_{44} & 0 & 0 \\ C_{13} & C_{23} & C_{33} & C_{34} & 0 & 0 \end{bmatrix}^k \tag{2b}$$

and the distributed force vector $\{p\}$ is

$$\{p\}^T=[p_r p_\theta p_z]. \tag{2c}$$

For definition and explanation of the quantities appearing in Eqs. (2a)–(b) the reader is again referred to Kohl *et al.*[26] The partition of the constitutive matrix in Eq. (2b), corresponding to the constitutive relations of Eq. (9) in Kohl *et al.*,[26] are for "cylindrically anisotropic"[27] media. This is the most general form of the constitutive relations considered. For materials which are transversely isotropic in the natural coordinate system of the cylinder, as the wires are considered here, $C_{56}=C_{34}=C_{24}=C_{14}=0$ and $C_{13}=C_{23}$.

For a pure axial pressure pulse, the impulse response is obtained using the boundary condition equation

$$\{p\}^T=[001]. \tag{3}$$

The integral on the left side of Eq.(2a) is the element contribution to an amplitude stiffness matrix. The integral on the right side of Eq. (2a) is the element contribution to a consistent nodal force vector. Assembly of the global stiffness matrix and consistent nodal force vector are done in the usual manner. The integrations of Eq. (2a) can be performed exactly for both solid and hollow cylinders.

As with traditional finite elements, either force or displacement may be specified on a node-by-node basis for each degree of freedom. The consistent nodal force vector represents a variational argument for node-by-node specification of force given prescribed surface traction. A solution using an unaltered amplitude stiffness matrix and consistent nodal force vector addresses the problem of a pure stress boundary condition problem. Such a solution is being examined here. Alternatively, using Eq. (2), in Kohl *et al.*,[26] evaluated at $z=0$, the nodal displacements for the $k$th element are given by

$$\{q(z,\omega)\}^{(k)}=[Q]^{(k)}\{A\}. \tag{4}$$

Nodal displacement is prescribed by replacing the row of the assembled global amplitude stiffness matrix corresponding to the displacement degree of freedom being specified with the appropriate row of $[Q]^{(k)}$ and replacing the same row entry of the consistent nodal force vector with the specified displacement.

For specific $\omega$, imposition of the boundary conditions of Eq. (3) and solution for the complex mode amplitudes $[A(\omega)]$ yields the impulse response $G(\omega)$ to a pure pressure pulse for any of the displacements, strains or stresses of interest. The time domain responses for any field variable, say $x(t)$, may be written as a convolution between the time domain impulse response $g(t)$ and the excitation that here is the prescribed pressure $p(t)$

$$x(t)=\int_0^t p(\lambda)g(t-\lambda)d\lambda. \tag{5}$$

The frequency domain transform of the field variable $x(t)$ is then given as $X(\omega)=G(\omega)P(\omega)$.

Considering the experimental configuration of Fig. 1, the analytical model is used to predict the waveform of the axial force resultant $[f_z=x(t)]$, or integral of the normal stress $\sigma_{zz}$ at the specimen end $z=L$, for comparison with experimental measurement. Given waveguide geometry and properties, the impulse response $[G(\omega)]$ for $f_z$ is computed at discrete frequencies over sufficient range so that all products $G(\omega)P(\omega)$ with significant amplitude are included in the computation. As discussed, the source waveform $p(t)$ is obtained by holding the generating and receiving transducers in face-to-face contact without the intervening waveguide. Fast Fourier transform (FFT) techniques are used to obtain $P(\omega)$. An inverse FFT of the product $F_z(\omega)=G(\omega)P(\omega)$ yields $f_z=x(t)$. Or the source $p(t)$ can be extracted from the measured axial force resultant $f_z$ using an inverse FFT of the quotient $P(\omega)=F_z(\omega)/G(\omega)$.

## V. PHASE VELOCITY MEASUREMENT AND MATERIAL PROPERTY CHARACTERIZATION

Effective implementation of the pulse propagation model requires accurate material characterization. The method of phase spectral analysis, given by Sachse and Pao,[25] is used with slight modification to measure phase velocity of the first longitudinal axisymmetric mode in thin wires over a 1–6 MHz range of frequency. Together with measurement of the first axially symmetric torsional mode, three of the five independent material properties for transversely isotropic media could be determined.

Measurement of the cylindrical guided wave velocity by phase spectral analysis requires measurement of an ultrasonic field at two axial locations. Assuming a single mode is associated with the measured signal, an ultrasonic field, $x(t,z)$, due to plane harmonic waves, can be written in the frequency domain as $x(\omega,z)=A(\omega)e^{-i\beta(\omega)z}$. The phase velocity $c=\omega/\beta$ is related to the phase $\phi$ of the quotient of the Fourier transforms of the two time domain samples of the ultrasonic field at the axial locations $z_1$ and $z_2$ according to

$$c(\omega)=\frac{\omega(z_2-z_1)}{\phi+2N\pi}, \tag{6a}$$

$$\phi(\omega)=\tan^{-1}\left(\frac{\mathrm{Im}(x(\omega,z_1)/x(\omega,z_2))}{\mathrm{Re}(x(\omega,z_1)/x(\omega,z_2))}\right). \tag{6b}$$

With the geometrical constraints of the measurement system shown in Fig. 1, measurement of the ultrasonic field after propagation in the sample is only possible at $z=L$. The transducers placed in face-to-face contact, without the intervening wire specimen, is taken as the ultrasonic field at $z=0$. The integer $N$ in Eq. (6a) is the integral number of wavelengths contained in the length of the wire specimen, when $\phi$ is constrained to the range 0 to $2\pi$.

From Eq. (6a), the phase velocities $(c_1,c_2)$ and phases $(\phi_1,\phi_2)$ at closely spaced frequencies $\omega_1$ and $\omega_2$ are related to $N$ by

$$N=\frac{\omega_1\phi_2-\omega_2\phi_1}{2\pi(\omega_2-\omega_1)}+\frac{(c_2-c_1)}{2\pi(z_2-z_1)}\frac{[\phi_1\phi_2+2N\pi(\phi_1+\phi_2)+4N^2\pi^2]}{(\omega_2-\omega_1)}. \tag{7}$$

As discussed, the first longitudinal mode tends toward nondispersiveness at low frequency. Nondispersive pulses propagate without distortion of the waveform envelope, and without change in the location of carrier frequency phase points within the envelope. A nondispersive or constant phase velocity approximation for $N$ neglects the second right-side term. This approximation error term clearly decreases for smaller $N$, which also occurs at low frequency. By transmitting a sufficiently low-frequency toneburst pulse, an accurate value for $N$ at the burst center frequency can be determined using this approximation.

Bursts are transmitted and the phase $\phi$ measured while the center frequency of the pulse is incremented. Only the phase information at the dominant frequency of a particular pulse is used. By incrementing the pulse center frequency in sufficiently small steps, the phase wrap (jumps between upper and lower limits of constrained phase) can be accurately tracked and the $N$ incremented very precisely. Given an accurate value for $N$ at the low starting frequency, $N$ can be determined unambiguously over the entire frequency range of measurement. Thereby, the phase velocity is determined discretely as a function of frequency, using Eq. (6a). The range of measurement can be extended up to frequencies where interference from other excited modes occurs or where the pulse becomes so dispersive that interference between multiple reflections of the same mode occurs.

This method was found to be more reliable than phase unwrapping,[25] wherein the constrained phase $(\phi)$ is examined from zero frequency to the frequency of interest. Each jump from $2\pi$ to 0 indicates that $N$ be incremented by 1. However, only with the capability to move the measurement points for the phase spectral analysis into close proximity, is sufficient *a priori* knowledge available to determine $N$ by phase unwrapping. When the measurement points are fixed and $N$ necessarily is large, the density of the phase jumps

TABLE I. List of measured material properties.

| Wire type (diameter and density) | $E_{LL}$ (GPa) | $\nu_{LT}$ | $G_{LT}$ (GPa) | $G_{iso}$ (GPa) |
|---|---|---|---|---|
| 304 stainless steel | | | | |
| 406 $\mu$m (16 mil), 7919 kg/m$^3$ | 211 | 0.30 | 74.5 | 81 |
| 305 $\mu$m (12 mil), 7852 kg/m$^3$ (annealed) | 208 | 0.30 | 76.0 | 80 |
| 127 $\mu$m (5 mil), 7913 kg/m$^3$ | 225 | 0.35 | 71.1 | 82 |
| aluminum 1100 | | | | |
| 406 $\mu$m (16 mil), 2679 kg/m$^3$ | 72.8 | 0.36 | 24.4 | 27 |
| 305 $\mu$m (12 mil), 2668 kg/m$^3$ | 68.6 | 0.36 | 25.3 | 25 |
| 127 $\mu$m (5 mil), 2742 kg/m$^3$ | 71.0 | 0.40 | 26.0 | 25 |

increases. Most real dispersive pulses will have regions of frequency exhibiting nonphysically realizable phase ($\phi$) information (i.e., corresponding to negative group velocity), often concomitant with low-magnitude complex amplitude $A(\omega)$. With a high density of phase jumps and even small regions of inaccurate phase information, the phase wraps become impossible to accurately track.

As noted previously, curve fitting of measured phase velocities of the first longitudinal axisymmetric mode through variation of material properties allows complete material property characterization for waveguides of isotropic media.[22] The same method may be applied to transversely isotropic cylinders provided that $E_{LL}$ and $\nu_{LT}$ are taken as the independent properties to be varied in obtaining the curve fit. Phase velocity measurements from low frequency to frequencies evidencing significant dispersion (approaching the cutoff of the second longitudinal mode) are required for accurate determination of both material properties.

The lowest torsional axisymmetric mode is nondispersive, for both transversely isotropic and isotropic cylinders. This mode is sensitive only to $G_{LT}$ for transverse isotropy. Once the torsional wavepacket is identified, its velocity is measured by cross-correlation.[28]

Table I summarizes the properties obtained in this manner for six different wire types investigated. The final column for each wire gives the shear modulus which would be required to support the conclusion of isotropy given the values of $E_{LL}$ and $\nu_{LT}$ determined by longitudinal mode measurement. Comparing this value of shear modulus with that obtained by torsional mode measurement is a measure of the material anisotropy and supports the conclusion that transverse isotropy better corresponds to the material behavior than isotropy, particularly for the steel wires. However, there is good agreement between solutions for the dispersion relations using either Pochhammer's exact solution for isotropic media taking $E$ and $\nu$ as independent properties, or using the numerical method described above and the complete set of five independent properties. The implication is that determination of $G_{LT}$ was only of interest in verifying the anisotropy of the media, but this anisotropy has no significant effect on the first longitudinal mode behavior. Since the first longitudinal mode propagation was not sensitive to the exact values for $E_{TT}$ and $G_{TT}$, these were set equal to $E_{LL}$ and $G_{LT}$, respectively.

Figures 4 and 5 show measured longitudinal mode velocities and the curve fits obtained, for 16-mil (406 $\mu$m) and 5-mil (127 $\mu$m) diameter stainless steel wires, respectively. The entire frequency range for which data was taken was not necessarily used for each wire. The solid circles indicate phase velocity measurements at discrete frequencies used in the curve fit shown as a solid line. In Fig. 5, additional measurements not used in the curve fit are shown as squares.

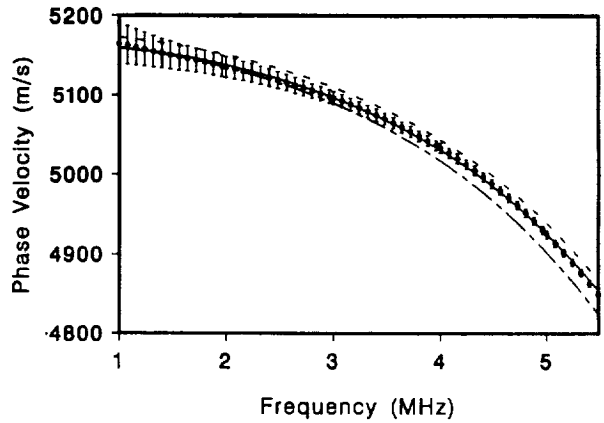


FIG. 4. Curve fit (solid line) of measured phase velocity (solid circles) to determine elastic properties for a 16-mil-diam 304 stainless steel wire. Analytical curves due to 0.5% increase in $E_{LL}$ (dotted line) and 5% increase in $\nu$ (dot–dash line) are also shown.

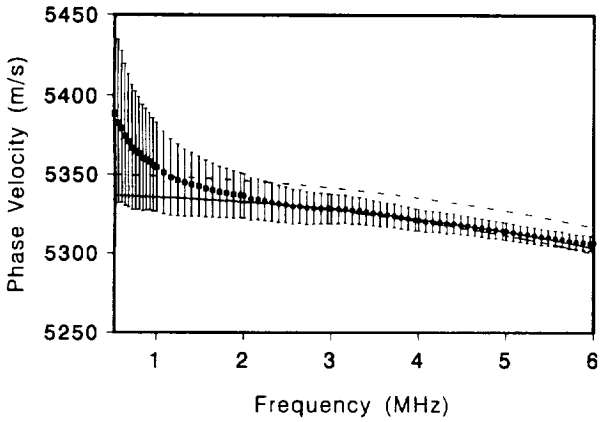


FIG. 5. Curve fit (solid line) of measured phase velocity (solid circles) to determine elastic properties for a 5-mil-diam 304 stainless steel wire. Analytical curves due to 0.5% increase in $E_{LL}$ (dotted line) and 5% increase in $\nu$ (dot–dash line) are also shown.

Additional information regarding error analysis and accuracy is also conveyed and requires some explanation.

The appearance of the measured dispersion at lower frequencies in Fig. 5 does not correspond to the first mode dispersion for any elastic cylinder. Such measurement anomaly was much more significant for the smaller diameter (127 $\mu$m) wires tested. The frequency dependences of transmission through both of the transducer/wire interfaces, which has been neglected, may plausibly be influenced by the wire diameter.

In general, several other factors may contribute to measurement error. First, the source waveform may be inadequately characterized, due to the difference in source transducer loadings between source measurement and transmission into the wire specimen. Furthermore, at the receiving end of the wire, some of the wave incident on the transducer is reflected, which may also give rise to some phase shift. The frequency difference between lower-measurement frequencies and the resonant frequency of the transducer (5 MHz) may exacerbate these problems.

If any resulting phase shift error at the pulse center frequency does not exceed some maximum value, say $\pi/2$, and the determination of $N$ remains unambiguous, it is clear from Eq. (6a) that the phase velocity measurement becomes more accurate as frequency increases. The actual phase ($\phi$) measurement becomes increasingly small relative to the quantity $2\pi N$ in the denominator of Eq. (6a). The error bars of Figs. 4 and 5 indicate the change in measured phase velocity which would result from a $\pm\pi/2$ shift in $\phi$.

Because of the apparent systematic error which occurred at lower frequencies for the 5-mil steel wire (Fig. 5), not all of the dispersive data available was used in the curve fit. That the analytical curve fit falls within the range of the error bars of the unused measurements for a $\pi/2$ maximum error in $\phi$, indicates that the phase shift error corresponds to less than a quarter of a wavelength. For the 16-mil diameter stainless steel wire (Fig. 4), measurements beyond 5 MHz were not used because of overlap and interference between longitudinal and flexural waves, as discussed previously.

The dashed lines of Figs. 4 and 5 show the alteration of

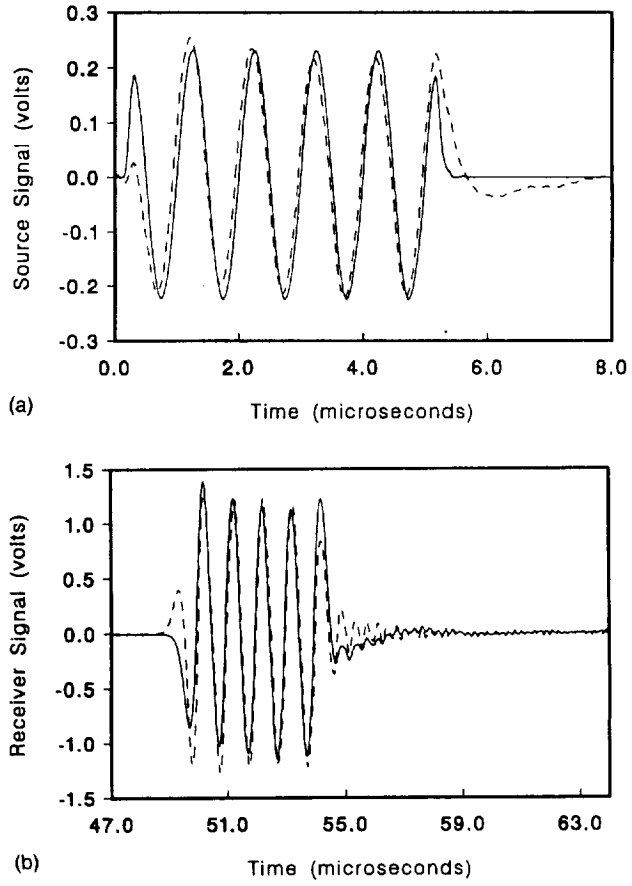


FIG. 6. Pulse propagation of a 1-MHz toneburst in 25.27-cm-long, 16-mil-diam 304 stainless steel wire; (a) measured (solid line) and analytically extracted (dashed line) source waveforms, (b) measured (solid line) and analytically predicted (dashed line) receiver waveforms.

the analytically determined curves due to 0.5% and 5% variations in $E_{LL}$ and $\nu_{LT}$, respectively. In comparing Figs. 4 and 5, specifically the dashed and solid curves in each figure, it is apparent that in order to determine $\nu_{LT}$ accurately, data associated with the increased dispersion at higher frequency, approaching the second longitudinal mode cutoff, must be available. Consequently, accuracy of the determination of $\nu_{LT}$ for the thicker wire was judged to be improved (i.e., the second mode cutoff is at much higher frequency for the thinner wire). The dispersion of the fundamental mode, as frequency and wire diameter to wavelength ratio increase, has been associated with the significance of radial inertia.[10,11] A conservative accuracy estimate of better than 0.5% for $E_{LL}$ and 5% for $\nu_{LT}$ is claimed when adequate dispersion measurements are available.

## VI. COMPARISON OF EXPERIMENTALLY MEASURED AND MODELED PULSE PROPAGATION

Comparison of experimentally measured receiver waveforms with analytically predicted responses, due to various measured sources, for the 16-mil steel wire, are shown in Figs. 6(b), 7(b), 8(b), and 9(b). The measured sources engendering these responses are shown in Figs. 6(a), 7(a), 8(a), and 9(a) together with the source waveform extracted from the aforementioned measured receiver waveforms. The analyti-

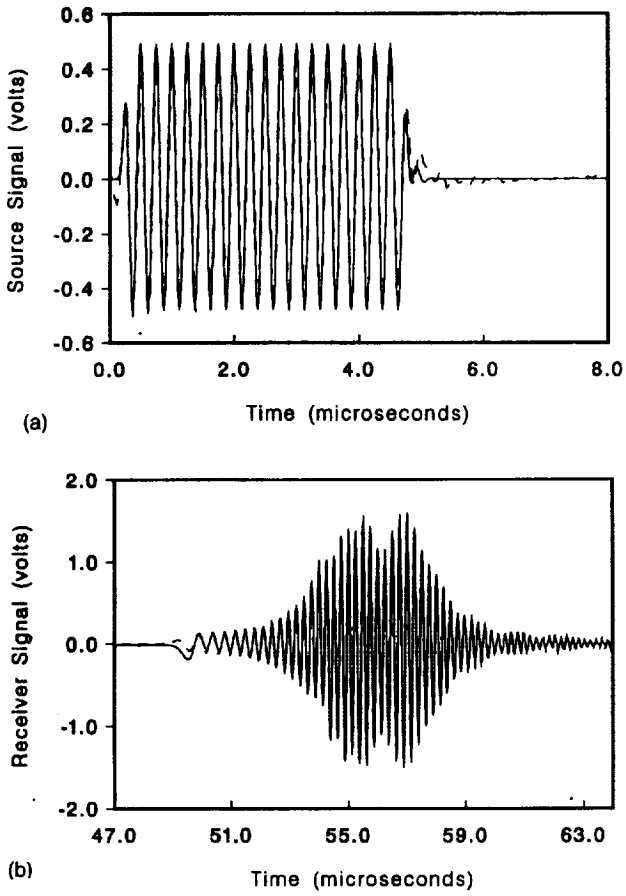


FIG. 7. Pulse propagation of a 4-MHz toneburst in a 25.27-cm-long, 16-mil-diam 304 stainless steel wire; (a) measured (solid line) and analytically extracted (dashed line) source waveforms, (b) measured (solid line) and analytically predicted (dashed line) receiver waveforms.

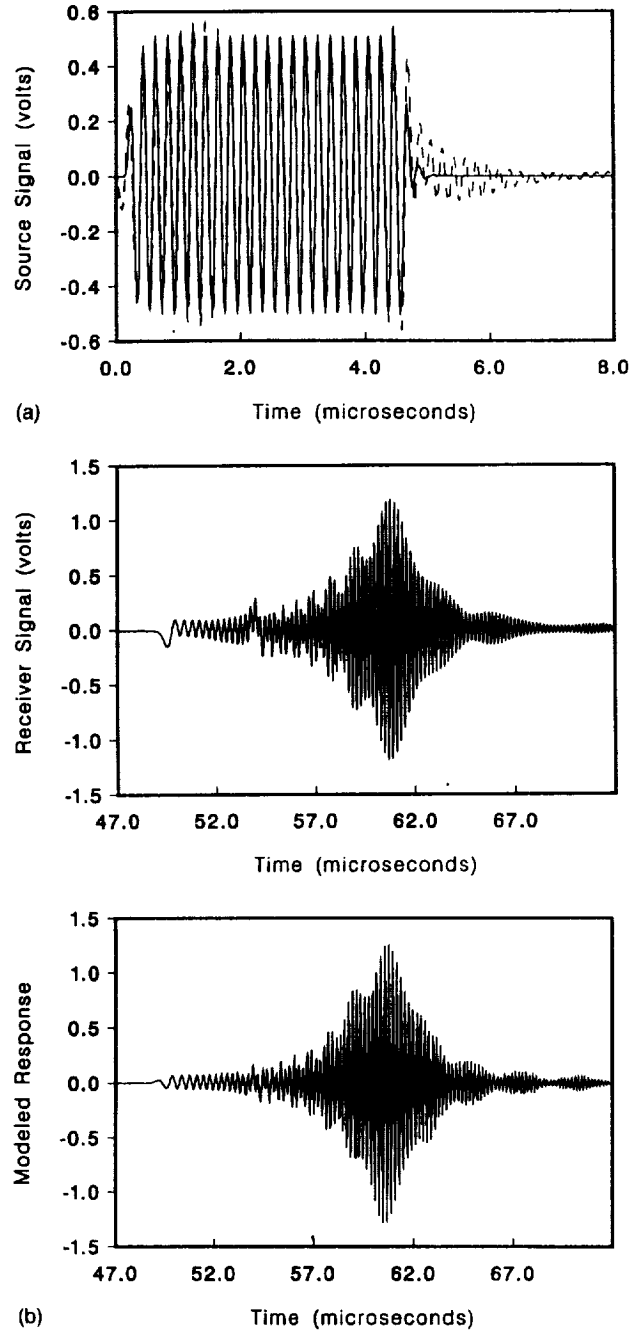


FIG. 8. Pulse propagation of a 5-MHz toneburst in a 25.27-cm-long, 16-mil-diam 304 stainless steel wire; (a) measured (solid line) and analytically extracted (dashed line) source waveforms, (b) measured (top) and analytically predicted (bottom) receiver waveforms.

cally determined responses and sources have been rms normalized with the measurements they are compared with. The source excitations for Figs. 6, 7, and 8 would be described as relatively narrow band pulses with increasing center frequency (1, 4, and 5 MHz, respectively), and with concomitantly increasing evidence of dispersion in the resulting response waveforms. These pulses are comparable to the pulses used to measure phase velocities and determine properties. Correspondence in measured and analytical sources and receivers is reasonable, even for the highly dispersive propagation exhibited in Fig. 8.

The efficacy of applying a semi-infinite waveguide model to propagation in samples which actually have boundaries, and consequently reflected waves at the end $z=L$, should be explained. The measured response at $z=L$ is due to both the incident and reflected waves, but only the incident waves are being used in the propagation model. However, provided that the reflected wave does not give rise to significant change in the phase of the measured response for a particular frequency harmonic and the reflection coefficient is constant as a function of frequency over the pulse bandwidth, the pulse waveform will not distort due to the presence of the reflected waves. Similarly, the presence of material attenuation and the lack of consideration given to the material attenuation in the model does not give rise to significant discrepancies between the measured and modeled response, provided that the attenuation is relatively constant over the frequency range of the pulse bandwidth. Both the presence of reflected waves and material attenuation, under these conditions, affect the amplitude of the measured waves uniformly as a function of frequency. The appearance of the pulse waveform, within a multipicative constant, is not affected. Since the analytical response is rms normalized with the measured wave, these shortcomings in the model are not apparent.

Figure 9 shows the pulse propagation due to a broadband excitation of the source transducer resulting from input of an electrical spike. The pulse distortion is severe because

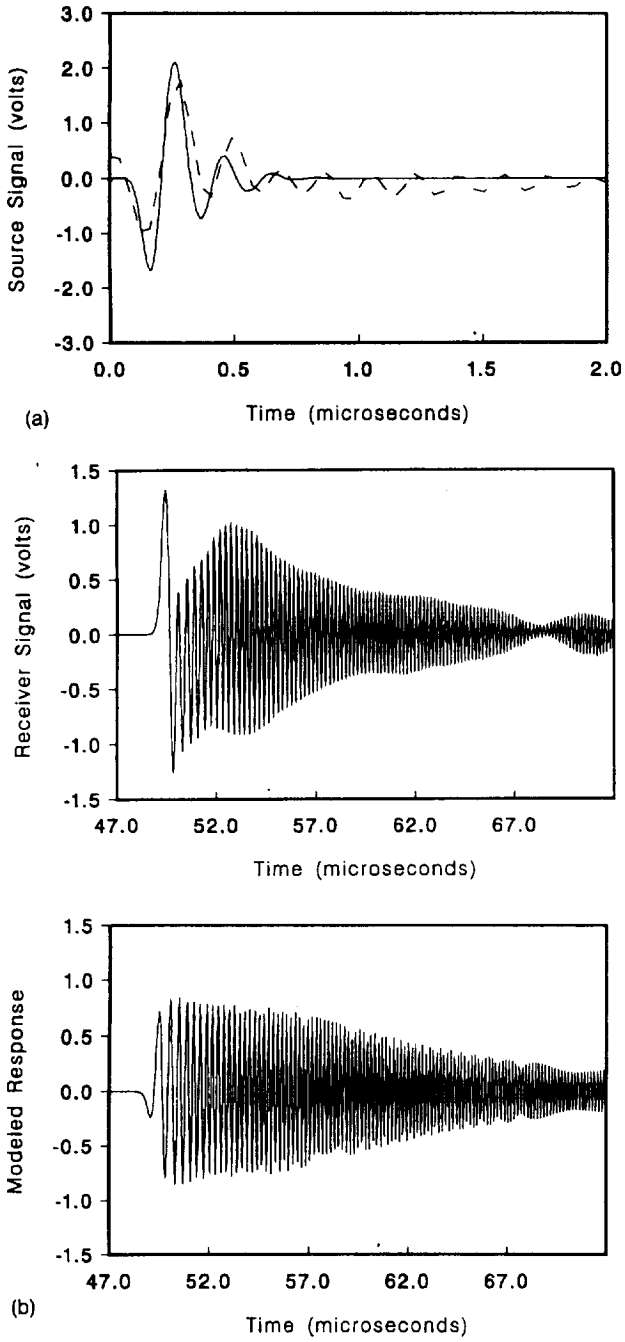


FIG. 9. Pulse propagation of a broadband pulse in a 25.27-cm-long, 16-mil-diam 304 stainless steel wire; (a) measured (solid line) and analytically extracted (dashed line) source waveforms, (b) measured (top) and analytically predicted (bottom) receiver waveforms.

of both the bandwidth and inclusion of higher-frequency components (transducer has 5-MHz resonant frequency). A consequence of this high level of dispersion is the lesser agreement between measured and predicted receiver waveforms. Inexactness in the source measurement, used to predict the response for a highly dispersive pulse, tends to be magnified in the response comparison. Reasonable agreement exists between measured and extracted source waveforms, despite the lesser agreement in response waveforms. To some extent the same conclusion can be drawn from Fig. 8, where the dispersion is lessened but still prevalent.

Waveforms comparing measured and modeled propagation of a 5-MHz center frequency narrowband pulse, in the 5 mil steel wire, are shown in Fig. 10. For the thinner wire and equivalent frequency excitations, much less dispersive pulse distortion is evident, reflecting the appearance of the dispersion curves in Figs. 4 and 5.

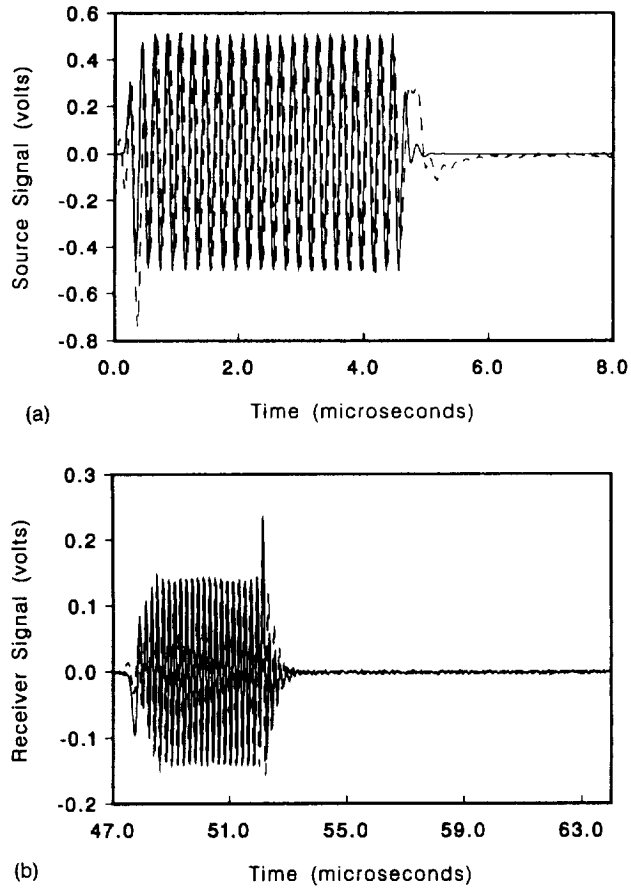


FIG. 10. Pulse propagation of a 5-MHz toneburst in a 25.22-cm-long, 5-mil-diam 304 stainless steel wire; (a) measured (solid line) and analytically extracted (dashed line) source waveforms, (b) measured (solid line) and analytically predicted (dashed line) receiver waveforms.

## VII. CONCLUSIONS

An analytical model of axially symmetric dispersive pulse propagation in cylinders with applied end conditions was experimentally investigated. Significant capability for modeling the generation and dispersive propagation of the fundamental longitudinal mode was demonstrated. Phase velocity measurement of the fundamental longitudinal and torsional axisymmetric modes were used to characterize material properties of the wires. Three of the five independent elastic properties for transversely isotropic media could be obtained, and the postulate of the nonisotropic nature of the drawn wires was supported. The method should be applicable to modeling the propagation of higher-order modes in solid cylinders, provided that the material is suitably characterized.

## ACKNOWLEDGMENTS

This work was supported in part by NASA Grant NAG-1-1390 and the George M. Low Fellowship, National Space Club.

[1] G. J. Curtis, "Wave Propagation Techniques in Determining the Dynamic Elastic Properties of Wires and Fibers," in *Ultrasonic Testing, Non-Conventional Testing Techniques*, edited by J. Szilard (Wiley, New York, 1982), pp. 555–598.

[2] L. C. Lynnworth, "Ultrasonic Measurement of Elastic Moduli in Slender Specimens Using Extensional and Torsional Wave Pulses," J. Test. Eval. **1**, 119–125 (1973).

[3] J. W. Ballou and S. Silverman, "Young's Modulus and Fibers and Films by Sound Velocity," J. Acoust. Soc. Am. **16**, 113–119 (1944).

[4] J. E. May, "Guided Wave Ultrasonic Delay Lines," in *Physical Acoustics*, edited by W. P. Mason (Academic, New York, 1964), Vol. IA, pp. 417–483.

[5] N. C. Nicholson and McDicken, W. N., "Waveguides in Medical Ultrasonics," Ultrasonics **26**, 27–30 (1988).

[6] C. V. O'Keefe, B. B. Djordjevic, C. G. Bouvler, and B. N. Ranganathan, "In-Situ Sensors and Structural Health Monitoring Applications," presented at Review of Progress in Quantitative NDE, 19–24 July 1992, San Diego, CA.

[7] L. Pochhammer, "Ueber die Fortpfanzungsgeshwindigkeiten Kleiner Schwingungen in einum unbregrenzien isotropen Kreiszylinder," Z. Math. **81**, 324–336 (1876).

[8] M. Onoe, H. D. McNiven, and R. D. Mindlin, "Dispersion of Axially Symmetric Waves in Elastic Rods," J. Appl. Mech. **29**, 729–734 (1962).

[9] I. Mirsky, "Wave Propagation in Transversely Isotropic Circular Cylinders Part I: Theory, Part II: Numerical Results," J. Acoust. Soc. Am. **37**, 1016–1026 (1965).

[10] R. D. Mindlin and H. D. McNiven, "Axially Symmetric Waves in Elastic Rods," J. Appl. Mech. **27**, 145–151 (1960).

[11] R. D. Mindlin and G. Herrmann, "A One-Dimensional Theory of Compressional Waves in an Elastic Rod," in *Proceedings of the First U. S. National Congress of Applied Mechanics*, June 1951 (ASME, New York, 1952), pp. 187–191.

[12] G. E. Hudson, "Dispersion of Elastic Waves in Solid Circular Cylinders," Phys. Rev. **63**, 46–51 (1943).

[13] L. Y. Tu, J. N. Brennan, and J. A. Sauer, "Dispersion of Ultrasonic Pulse Velocity in Cylindrical Rods," J. Acoust. Soc. Am. **27**, 550–555 (1955).

[14] J. Zemanek, "An Experimental and Theoretical Investigation of Elastic Wave Propagation in Cylinders," Doctoral dissertation, University of California, Los Angeles, CA (1962).

[15] N. C. Nicholson, W. N. McDicken, and T. Anderson, "Waveguides in Medical Ultrasonics: An Experimental Study of Mode Propagation," Ultrasonics **27**, 101–106 (1989).

[16] R. Skalak, "Longitudinal Impact of Semi-Infinite Circular Elastic Bars," J. Appl. Mech. **24**, 59–64 (1957).

[17] R. Folk, G. Fox, C. A. Shook, and C. W. Curtis, "Elastic Strain Produced by Sudden Application of Pressure to One End of a Cylindrical Bar," J. Acoust. Soc. Am. **30**, 552–563 (1958).

[18] J. Miklowitz and C. R. Nisewanger, "The Propagation of Compressional Waves in a Dispersive Elastic Rod, Part II–Experimental Results and Comparison with Theory," J. Appl. Mech. **24**, 240–244 (1957).

[19] D. Y. Hsieh and H. Kolsky, "An Experimental Study of Pulse Propagation in Elastic Cylinders," Proc. Phys. Soc. **71**, 608–612 (1958).

[20] H. D. McNiven and Y. Mengi, "Experimental Assessment of the Mindlin–McNiven Rod Theory," J. Acoust. Soc. Am. **62**, 589–594 (1977).

[21] T. Kohl, W. P. Rogers, and S. K. Datta, "Dispersive Pulse Propagation and Material Characterization for Hollow Cylindrical Waveguides," in Scientific and Engineering Aspects of Nondestructive Evaluation, *Proceedings of 1993 ASME Pressure Vessels and Piping Division Conference, NDE Engineering Division*, edited by M. N. Srinivasan (ASME, New York, 1993).

[22] T. R. Meeker and A. H. Meitzler, "Guided Wave Propagation," in *Physical Acoustics*, edited by W. P. Mason (Academic, New York, 1964), Vol. 1A, pp. 111–167.

[23] R. M. Christensen, *Mechanics of Composite Materials* (Wiley, New York, 1979), pp. 73–78.

[24] E. M. Young, "Discussion of Time Delay in Reference to Electrical Waves," IRE Trans. Ultrason. Eng. **UE-9**, 13–21 (1962).

[25] W. Sachse and Y. H. Pao, "On the Determination of Phase and Group Velocities of Dispersive Waves in Solids," J. Appl. Phys. **49**, 4320–4327 (1978).

[26] T. W. Kohl, S. K. Datta, and A.H. Shah, "Axially Symmetric Pulse Propagation in Semi-Infinite Hollow Cylinders," AIAA J. **30**, 1617–1624 (1992).

[27] K. H. Huang and S. B. Dong, "Propagating Waves and Edge Vibrations in Anisotropic Composite Cylinders," J. Sound Vib. **96**, 363–379 (1984).

[28] D. R. Hull, H. E. Kautz, and A. Vary, "Measurement of Ultrasonic Velocity Using Phase-Slope and Cross-Correlation Methods," Mater. Eval. **43**, 1455–1460 (1985).